

Diketopyrrolopyrrole-based oligomers accessed via sequential C–H activated coupling for fullerene-free organic photovoltaics

Shi-Yong Liu ^{a, b, *}, Wen-Qing Liu ^b, Cui-Xia Yuan ^b, Ai-Guo Zhong ^a, Deman Han ^a, Bo Wang ^b, Muhammad Naeem Shah ^b, Min-Min Shi ^{b, **}, Hongzheng Chen ^{b, ***}

^a Department of Pharmacy & Chemistry, Taizhou University, Taizhou, 317000, PR China

^b Department of Polymer Science & Engineering, Zhejiang University, Hangzhou, 310027, PR China

ARTICLE INFO

Article history:

Received 1 June 2016

Received in revised form

4 July 2016

Accepted 5 July 2016

Available online 7 July 2016

Keywords:

Diketopyrrolopyrrol (DPP)

Direct arylation

Atom economy

Non-fullerene acceptor

P3HT

Organic solar cell

ABSTRACT

Exploring sustainable chemistry for renewable energy plays a key role in meeting the ever increasing energy demand without sacrificing the environment. In this study, two novel diketopyrrolopyrrol(DPP)-based π -conjugated oligomers (named as **TPE-DPP₄** and **BP-DPP₄**) have been readily synthesized *via* a ligand-free Pd-catalyzed sequential activation of C–H bond in two steps with good yields starting from simple building blocks. Poly(3-hexylthiophene) is employed as an electron donor to blend with the new DPP-derived electron acceptors for the fullerene-free bulk heterojunction organic photovoltaics. The power conversion efficiency of 2.49% has been achieved, corresponding with an open-circuit voltage of 1.16 V, which is among the highest open-circuit voltages for the single-junction organic photovoltaics. The facilely accessible electron acceptors blended with cost-effective poly(3-hexylthiophene) donor for fullerene-free organic photovoltaics opens a new pathway to access renewable solar energy *via* sustainable chemistry.

© 2016 Elsevier Ltd. All rights reserved.

1. Introduction

Bulk heterojunction organic photovoltaics (BHJ OPV) has emerged as a promising renewable energy technology due to its merits of low-cost, light-weight, solution-processability and good flexibility [1–4]. Typically, the active layers of OPVs consist of fullerenes as electron acceptors (A) and conjugated (macro) molecules as electron donors (D) [5]. In spite of their widespread usage, fullerene-based acceptors do suffer from drawbacks including weak absorption of visible light, poor stability of morphology, limited chemical and electronic tunability, and high production cost, which may suppress the sustainability of OPV technology. In recent years, the conjugated semiconducting polymers and oligomers [6], which possess broad tunability in all the aspects of light absorption, frontier orbital energy levels (FOEL), electron affinity, molecular geometry and synthetic complexity, have been explored

as electron acceptors in place of fullerenes for BHJ OPVs [7–14]. These fullerene-free OPVs have raised extensive attention and led to a rapid progress very recently [15–22], e.g., the indacenodithieno[3,2-b]thiophene-2-(3oxo-2,3-dihydroinden-1-ylidene)malononitrile (ITIC) acceptor developed by the Zhan group [15]. Nevertheless, to ensure the cost-effectiveness and sustainability of fullerene-free OPVs, the accessibility of both acceptor and donor materials need to be carefully evaluated [23–25]. Green and sustainable synthetic strategies [26–39] to the π -conjugated materials using readily available building blocks are favorable to reach the above goal [23]. Moreover, the use of commercially available and well-developed semiconducting materials with relatively low price is recommendable [23–25].

In the current work, two novel DPP-based oligomer acceptors have been designed and synthesized *via* direct arylation of C–H bond (DACH) to pair with polymeric donor P3HT for fullerene-free BHJ OPV applications. Concerning the sustainability, this P3HT-DPPs donor-acceptor combination has some distinct advantages. DPP is not only a commercialized dye chromophore [40], but also a sustainable and readily available building block for the organic semiconducting materials [41–44]. Previous investigation shows that DPP unit is among the most synthetically accessible electron-poor monomers due to its low synthetic complexity [23]. Also, as

* Corresponding author. Department of Pharmacy & Chemistry, Taizhou University, Taizhou, 317000, PR China.

** Corresponding author.

*** Corresponding author.

E-mail addresses: chelsy@zju.edu.cn (S.-Y. Liu), [\(M.-M. Shi\)](mailto:minminshi@zju.edu.cn), [\(H. Chen\)](mailto:hzchen@zju.edu.cn).

demonstrated by our previous study, the accessibility of DPP derivatives can be further increased by employing the atom-efficient C–H activation reaction [45]. As for the donor applied herein, P3HT is one of the most frequently studied 2nd generation semiconducting polymers, which has a relatively lower price compared with other high performance 3rd generation D–A semiconducting polymers [25,46]. It is known that P3HT donor has a wide bandgap, and high-lying LUMO (lowest unoccupied molecular orbital) and HOMO (highest occupied molecular orbital) levels. Meanwhile, the conjugated polymers or oligomers containing a DPP block typically have narrow or medium bandgaps with higher LUMO levels compared to the commonly-used acceptors such as PC₆₁BM or perylene diimide (PDI) which has four electron-withdrawing carbonyl groups [47,48]. Therefore, the P3HT-DPP BHJ OPVs are expected to achieve high open-circuit voltages (V_{OC}) and a broad range of light harvesting, due to the enlarged gap between LUMO of DPP and HOMO of P3HT, and the complementary light absorptions of the wide-bandgap P3HT and narrow-bandgap DPPs [49–53].

Taking all of the abovementioned aspects into account, two novel non-planar oligomers both containing four DPP blocks have been design and synthesized in good yields by direct arylation of mono-phenyl capped DPP respectively using tetrakis(4-bromophenyl)ethene (TBPE) and tetrabromo-biphenyl (TBBP) as arylating reagents. From the viewpoint of molecular design, the twisted non-planar [20–22,54,55], quasi-3D [56] and 3D [52,53,57–59] molecular acceptors suggest that the optimization of the morphology of BHJ layer and thus fill factors (FF) can be realized by molecular geometry engineering. Tetraphenylethene (TPE) has been widely used as a building block in the field of aggregation-induced emission (AIE) [60,61] and very recently as a core for PDI-based 3D non-fullerene acceptor [54]. In this study, for the first time, the TPE and biphenyl (BP)-cored tetra-DPP (named as **TPE-DPP₄** and **BP-DPP₄**, Scheme 1) have been easily obtained via sequential C–H activation starting from simple building blocks. To the best of our knowledge, there are no previous reports using strategy of sequential C–H activation for accessing structurally complicated DPP-based oligomers. The non-planar conjugated oligomers obtained herein were further evaluated as non-fullerene acceptors in BHJ OPVs by using cost-effective P3HT as donor, affording a highest PCE of 2.49% with an open-circuit voltage (V_{OC}) of 1.16 V, which is among the highest V_{OC} for the single-junction OPVs reported. The integration of easily accessible acceptors with an economical donor for fullerene-free OPVs provided by us represents a step toward accessing renewable solar energy by sustainable chemistry.

2. Experimental section

The general synthetic routes toward Ph-DPP, **TPE-DPP₄** and **BP-DPP₄** are outlined in Scheme 1. The detailed synthetic procedures are as follows.

2.1. Synthesis of Ph-DPP

DPP (1000 mg, 524.78, 1.90 mmol), PivOH (60 mg, 0.3 equiv.), and anhydrous K₂CO₃ (316 mg, 1.2 equiv.) were added into a Schlenk tube. The mixed solid in the tube was purged by repetitions of vacuum and nitrogen filling (×3). Then a mixture of bromobenzene (300 mg, 1.90 mmol) and an anhydrous DMA (25 mL) solution of Pd(OAc)₂ (8 × 10⁻⁵ M) was added into the tube. The reaction solution was put through freeze-vacuum-thaw cycles three times to remove dissolved gases, and then rigorously stirred at 110 °C for 10 h under nitrogen atmosphere. After cooling to room temperature, the mixture was poured into an aqueous solution of NaCl (saturated, 250 mL) to remove the high boiling point solvent

DMA. The precipitate was extracted with CH₂Cl₂ (3 × 40 mL). The combined organic layer was washed with distilled water. Removal of the solvent by rotary evaporator afforded the crude product, which was then purified by column chromatography on silica gel using the mixtures of CH₂Cl₂ and hexane as eluent (1.5:1, v/v) and gave a deep red solid (790 mg, 70%). The thin layer chromatography (TLC) analysis for the reaction is shown in Fig. S1 (see Supplementary Information, SI). Ph-DPP is a known compound [45].

¹H NMR (500 MHz, CDCl₃) δ 8.97 (d, J = 4.0 Hz, 1H), 8.89 (d, J = 3.5 Hz, 1H), 7.68 (d, J = 7.5 Hz, 2H), 7.62 (d, J = 5.0 Hz, 1H), 7.42 (ddd, J = 5.0, 6.5, 4.0 Hz, 4H), 7.30–7.27 (m, 1H), 4.16–3.89 (m, 4H), 1.93 (d, J = 5.5 Hz, 2H), 1.37–1.25 (m, 16H), 0.88 (ddd, J = 5.5, 6.0, 3.5 Hz, 12H).

2.2. Synthesis of **TPE-DPP₄**

Ph-DPP (300 mg, 0.5 mmol), 1,1,2,2-tetrakis(4-bromophenyl)ethene (TBPE) (65 mg, 0.1 mmol), PivOH (15 mg, 0.15 mmol), and anhydrous K₂CO₃ (83 mg, 0.6 mmol) were added into a Schlenk tube. The mixed solid in the tube was purged by repetitions of vacuum and nitrogen filling (×3). Then 10 mL anhydrous DMA solution of Pd(OAc)₂ (5 × 10⁻⁵ M) was added into the tube via syringe. The reaction solution was put through freeze-vacuum-thaw cycles three times to remove dissolved gases, and then rigorously stirred at 110 °C for 10 h under nitrogen atmosphere. The post-treatment of the reaction are similar to that of Ph-DPP. The crude product was purified by column chromatography on silica gel using the mixtures of CHCl₃ and ethyl acetate (EA) as eluent (100:1, v/v) and gave a dark blue solid (235 mg, yield 86%, calculated from TBPE).

¹H NMR (600 MHz, CDCl₃) δ 8.93 (dd, J = 11.4, 4.2 Hz, 8H), 7.64 (d, J = 7.5 Hz, 8H), 7.49 (d, J = 8.1 Hz, 8H), 7.37 (dd, J = 38.7, 7.3 Hz, 20H), 7.13 (d, J = 7.7 Hz, 8H), 4.04 (s, 16H), 1.91 (s, 8H), 1.30 (d, J = 68.0 Hz, 65H), 0.86 (dd, J = 34.4, 15.3 Hz, 48H).

¹³C NMR (151 MHz, CDCl₃) δ 164.26, 152.32, 152.56, 146.39, 142.54, 142.23, 139.52, 135.77, 134.98, 134.45, 131.77, 131.51, 128.72, 128.20, 127.05, 111.01, 110.78, 48.61, 41.96, 32.99, 31.25, 26.33, 25.86, 16.71, 13.26.

MALDI-TOF MS (*m/z*): [M]⁺ calcd for C₁₇₀H₁₈₈N₈O₈S₈, 2727.90; found, 2728.42. Elemental Anal.: calcd: C, 74.85; H, 6.95; N, 4.11. Found: C, 74.86; H, 6.95; N, 4.12.

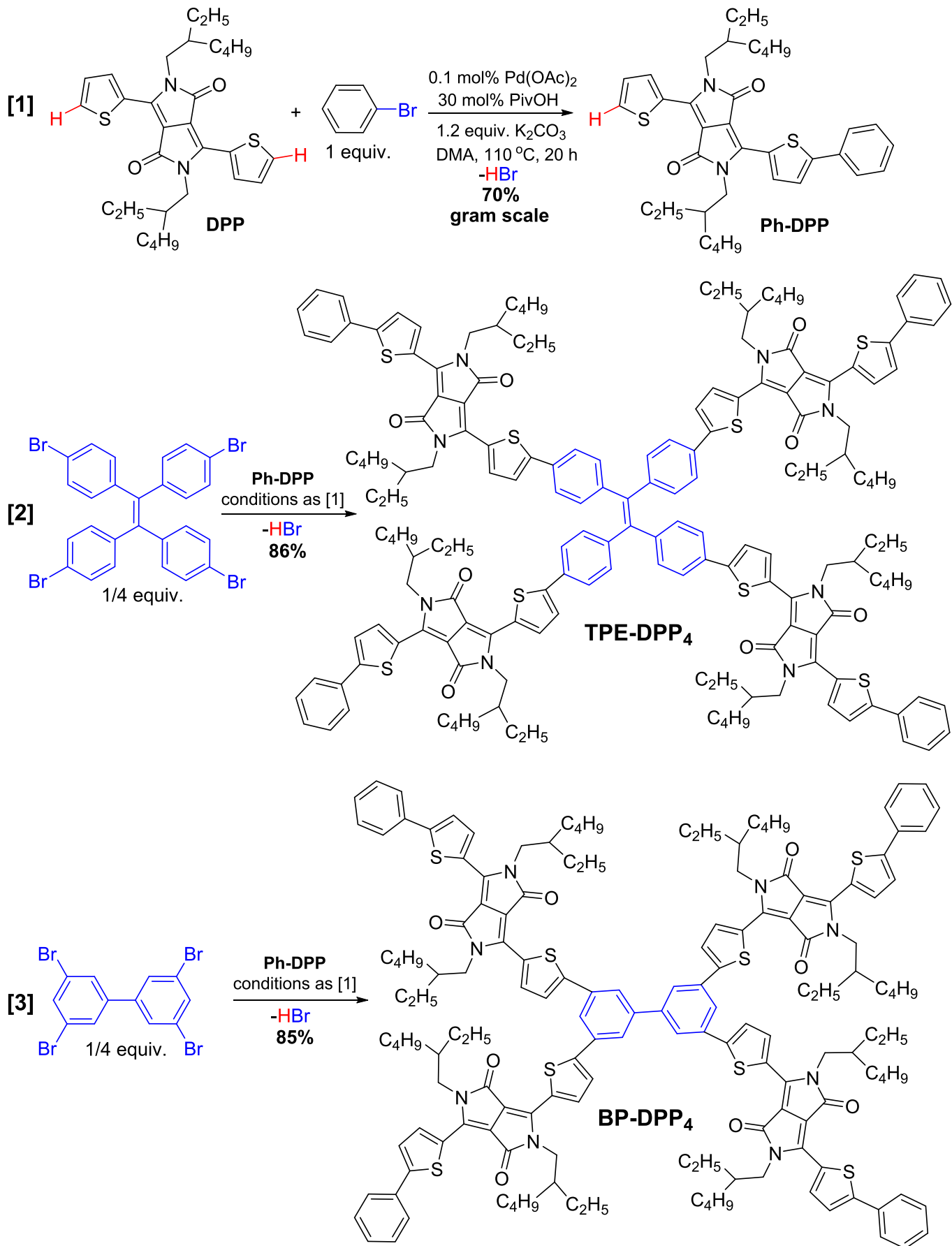
2.3. Synthesis of **BP-DPP₄**

Ph-DPP (300 mg, 0.5 mmol), 3,3',5,5'-tetrabromo-1,1'-biphenyl (TBBP) (47 mg, 0.1 mmol), PivOH (15 mg, 0.15 mmol), and anhydrous K₂CO₃ (83 mg, 0.6 mmol) were added into a Schlenk tube. The mixed solid in tube was purged by repetitions of vacuum and nitrogen filling (×3). Then an anhydrous DMA (10 mL) solution of Pd(OAc)₂ (5 × 10⁻⁵ M) was added into the tube via syringe. The reaction solution was put through freeze-vacuum-thaw cycles three times to remove dissolved gases, and then rigorously stirred at 110 °C for 10 h under nitrogen atmosphere. The post-treatment of the reaction are similar to that of Ph-DPP. The crude product was purified by column chromatography on silica gel using the mixtures of CHCl₃ and ethyl acetate (EA) as eluent (100:1, v/v) and gave a dark blue solid (216 mg, yield 85%, calculated from TBBP).

¹H NMR (600 MHz, CDCl₃) δ 9.00 (s, 8H), 7.82 (d, J = 26.8 Hz, 6H), 7.56 (m, 12H), 7.33 (m, 16H), 3.98 (s, 16H), 1.90 (s, 8H), 1.31 (d, J = 78.8 Hz, 64H), 0.80 (d, J = 77.5 Hz, 48H).

¹³C NMR (151 MHz, CDCl₃) δ 168.32, 163.96, 163.74, 152.46, 144.92, 140.06, 137.47, 135.68, 133.54, 132.53, 131.84, 131.28, 128.48, 126.99, 111.23, 110.32, 110.09, 48.62, 42.01, 32.46, 32.02, 31.28, 29.93, 26.36, 25.77, 16.78.

MALDI-TOF MS (*m/z*): [M]⁺ calcd for C₁₅₆H₁₇₈N₈O₈S₈, 2549.67;

**Scheme 1.** Sequential Activation of C–H Bonds for Accessing **TPE-DPP₄** and **BP-DPP₄**.

found, 2550.33. Elemental Anal.: calcd: C, 73.49; H, 7.04; N, 4.39. Found: C, 73.47; H, 7.05; N, 4.40.

2.4. Device fabrication and characterization

OPV devices were fabricated on glass substrates commercially pre-coated with a layer of ITO. Prior to fabrication, the substrates were cleaned using detergent, de-ionized water, acetone, and isopropanol consecutively for every 15 min, and then treated in an ultraviolet ozone generator for 15 min before being spin-coated at 3000 rpm with a layer of 30 nm thick poly(3,4-ethylenedioxythiophene):poly(styrenesulfonate) (PEDOT:PSS). After baking the PEDOT:PSS layer in air at 150 °C for 15 min, the substrates were transferred to a glovebox. The active layer was spin-cast at 3000 rpm from a solution of P3HT and the tetra-DPPs in chloroform with different blend weight ratios at a total solid concentration of 15 mg ml⁻¹. The samples might be annealed at 110 °C for 10 min. Then a 5 nm thick poly [(9,9-bis(3'-(N,N-dimethylamino) propyl)-2,7-fluorene)-alt-2,7-(9,9-diethylfluorene)] (PFN) film was deposited as the cathode buffer layer by the spin-coating of a solution of 0.4 mg ml⁻¹ PFN in methanol because PFN could reduce greatly the work function of the cathode, in favor of electron collection in the OPVs. Subsequently, the samples were loaded into a vacuum deposition chamber (background pressure ≈ 5 × 10⁻⁴ Pa) to deposit 100 nm thick aluminum cathode with a shadow mask (the device area was 5.2 mm²). The J-V curves were measured with a Keithley 2400 measurement source units at room temperature in air. The photocurrent was measured under a calibrated solar simulator (Abet 300W) at 100 mW cm⁻² and the light intensity was calibrated with a standard photovoltaic (PV) reference cell. IPCE spectra were measured with a Stanford lock-in amplifier 8300 unit. The charge carrier mobilities of the P3HT:tetra-DPPs films were measured using the SCLC method. Hole-only devices were fabricated in a structure of ITO/PEDOT:PSS/P3HT:tetra-DPPs(2:1)/MoO₃/Al, electron-only devices were fabricated in a structure of ITO/PFN/P3HT:tetra-DPPs(2:1)/PFN/Al. The device characteristics were extracted by modeling the dark current under forward bias using the SCLC expression described by the Mott-Gurney law:

$$J = \frac{9}{8} \epsilon_r \epsilon_0 \mu \frac{V^2}{L^3}$$

Here, $\epsilon_r \approx 3$ is the average dielectric constant of the blend film, ϵ_0 is the permittivity of the free space, μ is the carrier mobility, $L \approx 100$ nm is the thickness of the film, and V is the applied voltage.

3. Results and discussion

3.1. Synthesis and sustainability aspects

Scheme 1 depicts the synthetic routes to two DPP-based oligomers **TPE-DPP₄** and **BP-DPP₄**, and the detailed procedures are described in the Experimental Section. Firstly, a mono-phenyl capped DPP, Ph-DPP, was obtained by the direct arylation of one α -C–H bond on thiophene-flanked DPP with one equiv of bromobenzene. The reaction was run under simple and ligand-free conditions: 0.1 mol % Pd(OAc)₂, 30 mol % pivalic acid (PivOH), 1.2 equiv anhydrous K₂CO₃, and solvent *N,N*-dimethylacetamide (DMA) at 110 °C for 10 h. It is noteworthy that this reaction can be carried out on a gram scale to afford Ph-DPP in good yield (reaction [1] in **Scheme 1**). After that, further arylation of the remaining α -C–H bond on Ph-DPP by multibromo-arenes, TBPE and TBBP, led to formation of TPE and BP cored tetra-DPPs, *i.e.* **TPE-DPP₄** and **BP-DPP₄** respectively. Overall, both oligomers were accessed by

sequential C–H activation of thiophene-flanked DPP in two steps with a global yield of more than 60% (70 % × 86 %). As shown in the reactions of [2] and [3] (**Scheme 1**), four DPP blocks were smoothly installed onto TPE or BP cores in one step simply starting from Ph-DPP, and TBPE or TBBP. Throughout the synthetic route, C–H and C–Br bonds were exclusively used as reactive sites to build new C–C bonds. Neither organometallic reactants (*e.g.*, organoborons, organotins and organozincs) nor strong bases (*e.g.*, LDA and BuLi) were employed. Besides, non-halogenated and non-aromatic solvent DMA was applied as reaction medium.

Concerning the sustainable chemistry, an efficient catalyst with high turnover number (TON, moles of substrate converted/moles of catalyst) will be highly desirable [62]. In our study, the DACH reactions were accomplished in a short time (10 h) in the presence of 0.1 mol % Pd(OAc)₂ without using phosphine ligands (**Scheme 1**). This catalysis was simple but highly efficient. To precisely quantify the ultralow catalyst loading for the reactions, stock DMA solution of Pd(OAc)₂, rather than solid Pd(OAc)₂, was added into reaction mixtures by syringes (see Experimental Section). These ligand-free Pd(OAc)₂-catalyzed DACH reactions with ultralow loading of catalyst (0.1 mol %) have a higher TON by 1–2 orders of magnitude than that of typical C–M/C–X bonds cross-couplings which usually need 2.5–10 mol % ligand-stabilized palladium catalyst, *e.g.*, Pd(PPh₃)₄.

Supposing the typical cross-couplings are employed instead, the synthesis of **TPE-DPP₄** and **BP-DPP₄** will be tedious and less atom-efficient than the sequential C–H activation. As shown in **Scheme S1** (see SI), from the same building blocks, six steps in total would be required if Suzuki or Stille couplings were used. During these processes, *n*-BuLi strong base and organotin or organoboron reactants are needed [63] (**Scheme S1, SI**). This comparison shows that the synthetic strategy we developed is more straightforward with total two steps and single byproduct of HBr (**Scheme 1**). It should be noted that the current synthetic route also has an improvement in atom efficiency as compared with all our previous ones using Suzuki coupling of mono-Br-DPP with phenylboronic acid to prepare Ph-DPP (**Scheme S2, SI**) [45,64–66].

On the whole, the strategy of sequential C–H activation (**Scheme 1**) provided herein for accessing DPP-based π -functional materials have a number of advantages in terms of sustainability [62], including (1) straightforward synthesis from simple building blocks on gram scale in few steps within short reaction time, (2) simple and ligand-free catalysis with ultralow catalyst loading and high TON, (3) bypassing the use of organometallic reactant and dangerous strong base, (4) absence of active C–M bonds in the reactants, and thus high compatibility with functional groups, (5) non-halogenated and non-aromatic solvent used for the reactions, (6) simple byproduct of HBr only, and, last but not least, (7) the current strategy can be extended as a general and effective method for accessing complex DPP-based functional materials.

3.2. Characterization and theoretical calculation

The target oligomers, **TPE-DPP₄** and **BP-DPP₄**, were fully characterized by ¹H and ¹³C NMR, matrix-assisted laser desorption ionization time of flight (MALDI-TOF) mass spectroscopy (MS) and elemental analysis (spectra shown in SI). Both DPP-based oligomers are readily soluble in common organic solvents such as CHCl₃, CH₂Cl₂, tetrahydrofuran and dichlorobenzene due to the presence of solubilizing *N*-substituted 2-ethyl-hexyl chains. The thermal properties of **TPE-DPP₄** and **BP-DPP₄** were checked by thermogravimetric analysis (TGA, **Fig. S2**), which shows that both **TPE-DPP₄** and **BP-DPP₄** exhibit good thermal stability with 5% weight-loss temperatures (T_d) at 390 and 401 °C under N₂ atmosphere, respectively. Differential scanning calorimetry (DSC) was used to

study the crystallinity of **TPE-DPP₄** and **BP-DPP₄** (Fig. 1). The DSC scanning of **TPE-DPP₄** exhibits both weak crystalline melting and recrystallization peaks at 241.5 and 192 °C respectively. Under the similar DSC scans, neither melting nor recrystallization peaks could be observed for **BP-DPP₄**. These results suggest that **TPE-DPP₄** and **BP-DPP₄** are low-crystalline and non-crystalline, respectively.

The geometries of the oligomers **TPE-DPP₄** and **BP-DPP₄** have been calculated by density functional theory (DFT) method. As shown in Fig. 2a and b, the optimized geometries indicate that both **TPE-DPP₄** and **BP-DPP₄** are twisted and non-planar, which comes from the non-planar nature of TPE and BP cores, the steric effect among the DPP arms, and also the phenyl-thiophene linkages between cores and DPP blocks. The non-planar architecture of **TPE-DPP₄** and **BP-DPP₄** will suppress the intermolecular packing [58], which is responsible for their less crystalline solid state when compared to their planar counter parts. This is likely true as the linear/planar DPPBzFu has highly crystalline [67,68]. Although the DPP arms of these non-planar oligomers have less molecular orbital (MO) overlap, they are close to each other in space. The charges on **TPE-DPP₄** and **BP-DPP₄** can delocalize throughout the DPP arms, and can hop among each other. Taking advantage of the non-planar geometries, the distribution and transport of charges in multi-directions will lead to statistically better D-A charge separation and collection [66].

3.3. Optical and electrochemical properties

To evaluate potential applications for OPV, the optical and electrochemical properties of **TPE-DPP₄** and **BP-DPP₄** were investigated. Fig. 2d shows the normalized individual UV-vis absorption spectra of the DPP-acceptors, and the donor polymer P3HT from spin-coated films. **TPE-DPP₄** and **BP-DPP₄** films exhibit very similar absorption spectra, with peaks ($\lambda_{\text{max}}^{\text{f}}$) at 588 and 638 nm for **TPE-DPP₄** and 587 and 639 nm for **BP-DPP₄**. These peaks are red-shifted compared to their solution absorption spectra ($\lambda_{\text{max}}^{\text{s}}$, Fig. S3), which can be ascribed to the enhanced intermolecular interaction in the solid state of oligomers. The absorption band-edge of the cast films ($\lambda_{\text{edge}}^{\text{f}}$) for **TPE-DPP₄** and **BP-DPP₄** are 777 and 774 nm respectively, corresponding to the optical bandgaps (E_g^{opt}) of 1.59 and 1.60 eV. To maximize the light harvesting of BHJs, integrating electron donors and acceptors with complementary light absorption is highly desirable. As shown in Fig. 2d, P3HT film has an absorption peak at 523 nm, which is blue-shifted compared

with tetra-DPPs. The light absorption of P3HT donor and tetra-DPP acceptors complements each other quite well.

Besides light absorption, suitable FOEL gaps between donor and acceptor play an important role in driving photon-generated charge dissociation and determining the parameters of BHJ OPV devices. The FOELs of DPP-acceptors were electrochemically checked by cyclic voltammetry (CV) in CH_2Cl_2 solution (Fig. S4). The LUMO and HOMO are estimated from the $E_{1/2}$ values in solution, using the value of -5.1 eV for Fc/Fc^+ . Fig. 2e shows the FOELs of the P3HT donors and DPP-based acceptors. The FOELs of fullerene-based acceptor PC₆₁BM were illustrated for comparison purpose. Both **TPE-DPP₄** and **BP-DPP₄** exhibit very similar HOMOs and LUMOs. As illustrated in Fig. 2e, the gap between the LUMO of DPPs and the HOMO of P3HT (1.12 eV) is much larger than that between PC₆₁BM and P3HT (0.74 eV), benefiting high Vocs for the BHJ OPVs based on P3HT and DPPs. Notably, both of LUMO-LUMO (-2.74 eV vs -3.64 eV) and HOMO-HOMO (-4.76 eV vs -5.08 eV) offsets between P3HT donor and tetra-DPP acceptors are larger than 0.3 eV, which is favorable for either electron or hole transfer between D-A interfaces [69]. That is, due to the suitable FOELs, the electrons on P3HT will transfer onto tetra-DPPs while the holes on tetra-DPPs will transfer onto P3HT, thus potentially increasing the photo-generated current (Fig. S5, S1).

Table 1 summarizes the significant optical and electrochemical properties of P3HT donor and tetra-DPP acceptors.

3.4. P3HT:tetra-DPPs fullerene-free BHJ OPV performances

Motivated by the complementary absorption and well-matched FOELs between P3HT donor and tetra-DPP acceptors, the devices with a configuration of ITO/PEDOT:PSS/P3HT:tetra-DPPs/PFN/Al were fabricated to investigate the performances of solution-processed BHJ OPVs under the simulated AM 1.5 G irradiation with intensity of 100 mWcm⁻². The devices based on P3HT:tetra-DPPs BHJ processed by chloroform are firstly optimized with three sets of D(P3HT)/A(tetra-DPPs) ratios, i.e. 3:1, 2:1 and 1:1. It was found that D/A ratio of 2:1 can afford best performance after thermal annealing at 110 °C for 10 min. Without annealing, a low PCE of 0.20% with a V_{OC} of 1.23 V, a short current (J_{SC}) of 0.69 mA cm⁻², and an FF of 0.23 is obtained when the blend weight ratio of donor (P3HT) and acceptor (**TPE-DPP₄**) is 2:1 (Table S1, S1). After thermal annealing at 110 °C for 10 min, the device with the same D:A blend ratio can give a maximum PCE of 2.49% with a V_{OC} of 1.16 V, a J_{SC} of 4.55 mA cm⁻², and a FF of 0.47. The same trend was also found in the BHJ of P3HT:**BP-DPP₄**. By annealing treatment, the PCE of P3HT:**BP-DPP₄** BHJ can dramatically improved from 0.4% to 1.18% (Table S1). Fig. 3a shows the current density-voltage ($J-V$) characteristic curves of the optimal cells. The corresponding OPV parameters are summarized in Table 2. For P3HT-based fullerene-free OPVs, the distinct enhancement of PCE by annealing treatment was also observed by our group previously [52]. The thermal annealing may promote intermolecular $\pi-\pi$ stacking in P3HT:tetra-DPP BHJ films, leading to better charge transport and suitable phase separation, which are desirable for J_{SC} , FF and thus the PCE. Impressively, the V_{OC} of 1.16 V achieved herein represents one of the highest values for the single-junction OPVs [49–53,70–72]. The large offset between the LUMOs of tetra-DPPs and HOMO of P3HT (Fig. 2e) contributed to the high V_{OC} s.

3.5. IPCE measurements

To understand the photophysical properties, the IPCE (incident photon-to-current conversion efficiency) of the P3HT:tetra-DPPs BHJs were studied. Fig. 3b shows the IPCE spectra of the optimal OPV device. The calculated J_{SCs} from IPCE are 4.51 and

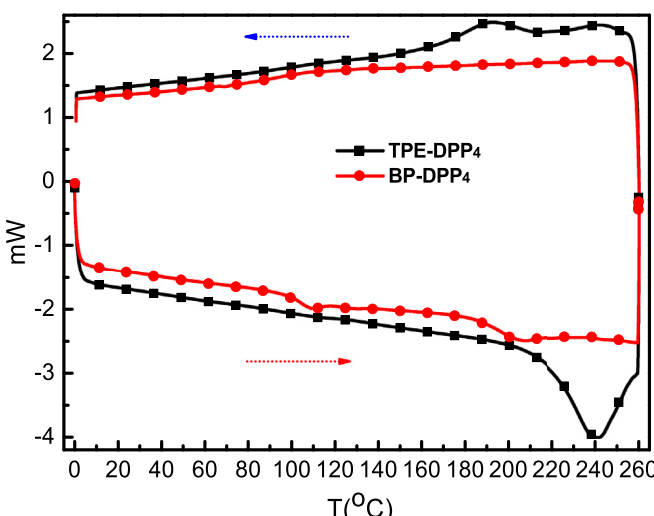


Fig. 1. DSC curves of **TPE-DPP₄** and **BP-DPP₄**.

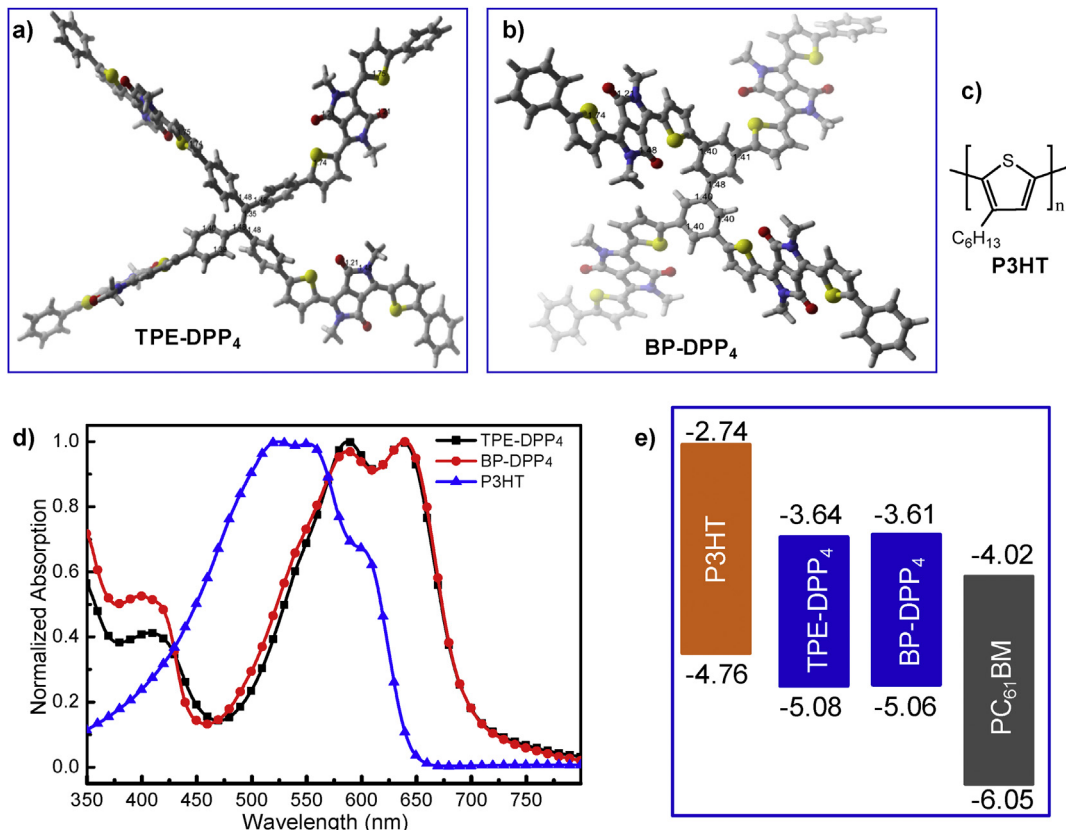


Fig. 2. DFT optimized geometries (ethyl-hexyl chains replaced by methyl groups) of (a) **TPE-DPP₄** and (b) **BP-DPP₄**. (c) Structure of P3HT. (d) UV-vis absorption of neat films of **TPE-DPP₄**, **BP-DPP₄** and P3HT. (e) FOEL diagram of P3HT, **TPE-DPP₄**, **BP-DPP₄** and PC₆₁BM.

Table 1

Optical and electrochemical properties of P3HT donor and tetra-DPP acceptors.

D or A	$\lambda_{\text{max}}^{\text{s}} \text{ (nm)}$	$\lambda_{\text{max}}^{\text{f}} \text{ (nm)}$	$\lambda_{\text{edge}}^{\text{f}} \text{ (nm)}$	$E_g^{\text{opt}} \text{ (eV)}$	HOMO (eV)	LUMO (eV)
P3HT	464	523	650	1.91	-4.76	-2.74
TPE-DPP₄	574/614	588/638	777	1.59	-5.08	-3.64
BP-DPP₄	569/608	589/639	774	1.60	-5.06	-3.61

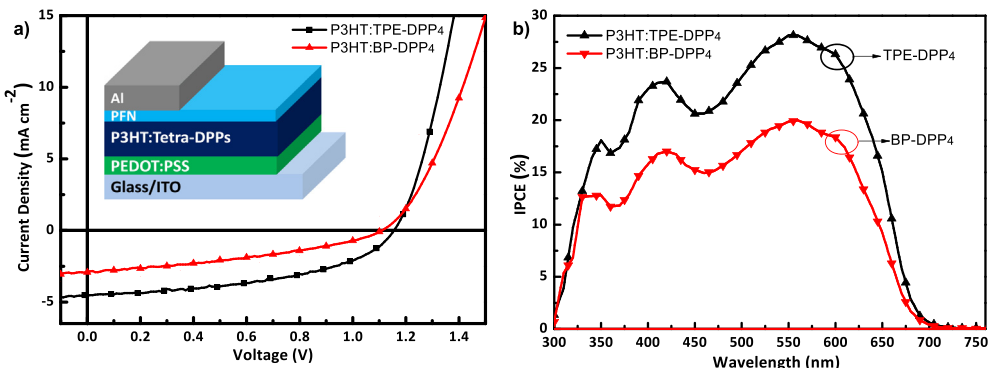


Fig. 3. (a) $J-V$ curves of P3HT:tetra-DPPs BHJs and their OPV device configuration. (b) IPCE spectra of P3HT:tetra-DPPs BHJs.

2.94 mA cm⁻², respectively, which are consistent with the measured J_{SC} s. Impressively, the IPCEs of P3HT:tetra-DPPs BHJs extend from 320 nm to 700 nm, matching well with their corresponding UV-vis absorption spectra (Fig. S3, SI). It indicates that light absorbed by both P3HT and tetra-DPPs were efficiently converted into current in solar cells, suggesting excitons generated

from donor and acceptor domain can be dissociated effectively at the D-A junction. The sufficient LUMO-LUMO and HOMO-HOMO offsets (>0.3 eV) between the donor and acceptor provided enough driving force for the photo-generated electron from P3HT transfer onto tetra-DPPs, while photo-generated hole from tetra-DPPs transfer onto P3HT (Fig. 2e and Fig. S5).

Table 2

Photovoltaic parameters of the OPV devices based on P3HT:tetra-DPPs.

D:A ^a	V _{OC} [V]	J _{SC} [mA cm ⁻²]	FF	PCE [%] ^d	μ_h [10 ⁻⁴ cm ² V ⁻¹ s ⁻¹] ^e	μ_e
P3HT:TPE-DPP ₄ ^b	1.23	0.69	0.23	0.20 (0.16)	1.24	0.23
P3HT:TPE-DPP ₄ ^c	1.16	4.45	0.47	2.49 (2.43)	1.41	0.32
P3HT:BP-DPP ₄ ^b	1.15	1.32	0.26	0.40 (0.37)	0.57	0.15
P3HT:BP-DPP ₄ ^c	1.11	2.93	0.36	1.18 (1.14)	0.87	0.17

^a The D:A ratio is 2:1 (w/w).

^b As-cast.

^c Annealed at 110 °C for 10 min.

^d The best and average (in brackets, from 10 devices) PCEs.

^e Hole and electron mobilities by SCLC method.

3.6. BHJ morphology and charge carrier mobility

Atomic force microscopy (AFM) and space-charge-limited-current (SCLC) measurements were employed to investigate surface morphology and charge mobility of the BHJ layers. AFM scans were carried out for films spin-coated on ITO substrates. Fig. 4 shows the AFM images of all the as-cast and annealing-treated P3HT:tetra-DPPs BHJs. In the as-cast films, P3HT is highly miscible with tetra-DPPs (Fig. 4a, c, e and g). The RMS roughness of the as-cast P3HT:TPE-DPP₄ and P3HT:BP-DPP₄ BHJs are 0.465 and 0.571 nm respectively. After thermal annealing, the RMS roughness of the BHJ films increases to 0.629 and 0.723 nm accordingly. It can be speculated that the thermal annealing helps to improve the phase separation, crystallinity, and domain purity [52]. For SCLC tests, all devices were fabricated by using the identical procedure for solar cell preparation. The J-V curves for hole-only and electron-only devices are shown in Fig. S7. The rightmost two columns in Table 2 list the corresponding values. As Table 2 shows, both hole mobility (μ_h) and electron mobility (μ_e) of P3HT:TPE-DPP₄ and P3HT:BP-DPP₄ BHJs are improved by thermal annealing treatment that leads to the enhanced crystallinity. In addition, the μ_h and μ_e of P3HT:TPE-DPP₄ BHJ are both higher than those of P3HT:BP-DPP₄ BHJ. Compared with BP-DPP₄, TPE-DPP₄ has a larger conjugation system and slightly higher crystallinity (Fig. S2), which may make contributions to the improved charge mobility.

4. Conclusion

Diketopyrrolopyrro (DPP), as a commercialized dye chromophore [40], is one of the most widely studied building blocks for organic semiconducting materials [41–44]. C–H is the most extensive chemical bond in organic compounds. The direct functionalization of C–H bonds for accessing target molecules has clearly attractive features for sustainable chemistry. In our work, starting from three simple building blocks, two large conjugated oligomers containing four DPP units have been readily constructed merely in two steps via Pd-catalyzed sequential arylation of C–H bonds. Neither organometallic reactants nor strong bases were employed throughout the processes of synthesis. The obtained DPP-based non-planar oligomers were tested as non-fullerene acceptors in OPVs by using commercially available P3HT as the donor, affording a best PCE of 2.49% with a high Voc of 1.16 V. The integration of easily accessible acceptors with economical donor for fullerene-free BHJ OPVs in our study represents a step toward accessing renewable solar energy via sustainable chemistry.

Importantly, the synthetic route developed herein can be extended as a general and effective method for accessing a wide number of DPP derivatives. Besides, the sequential C–H activation strategy for atom-efficient construction of π -conjugated oligomers should be applicable for other building blocks beyond DPP moiety. We believe, in the future, more and more π -semiconducting materials will be accessed via sequential C–H activation for organic electronic applications.

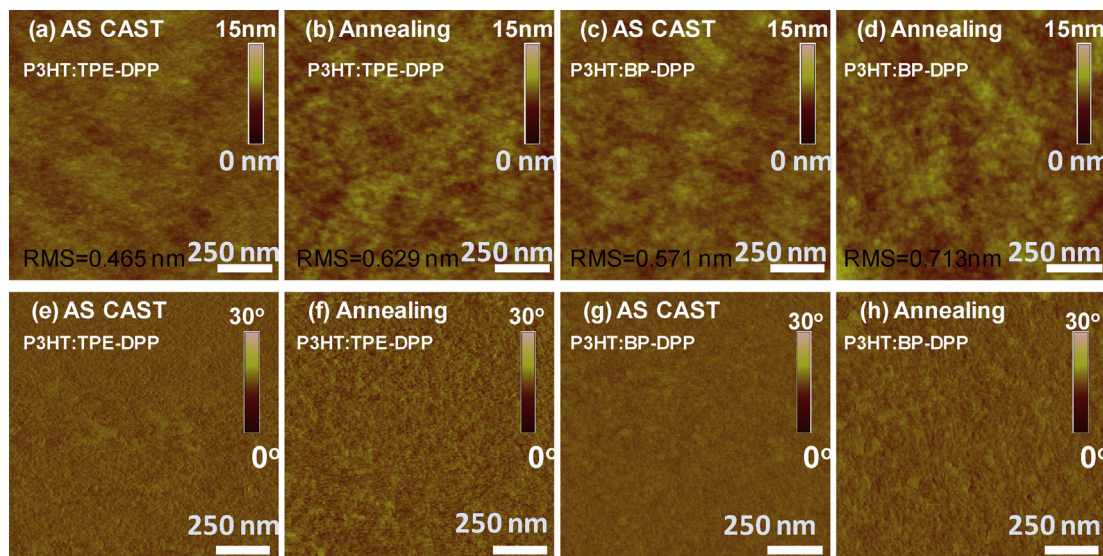


Fig. 4. AFM height (a, b, c, d) and phase (e, f, g, h) images of the P3HT:tetra-DPPs (2:1 by weight) BHJ films with or without annealing treatment.

Acknowledgements

The National Natural Science Foundation of China (21244008, 21374075, 21575097, 21375092), China Postdoctoral Science Foundation (Nos. 2013M540484 and 2014T70572), and Zhejiang Provincial Natural Science Foundation of China (No. LY15B030001) are appreciated for financial supports. SY Liu and WQ Liu contributed equally to this work.

Appendix A. Supplementary data

Supplementary data related to this article can be found at <http://dx.doi.org/10.1016/j.dyepig.2016.07.007>.

References

- [1] Hösel M, Angmo D, Søndergaard RR, dos Reis Benatto GA, Carlé JE, Jørgensen M, et al. High-volume processed, ITO-free superstrates and substrates for roll-to-roll development of organic electronics. *Adv Sci* 2014;1:1400002.
- [2] Berny S, Blouin N, Distler A, Egelhaaf HJ, Krompiec M, Lohr A, et al. Solar trees: first large-scale demonstration of fully solution coated, semitransparent, flexible organic photovoltaic modules. *Adv Sci* 2016;3:1500342.
- [3] Li Y. Molecular design of photovoltaic materials for polymer solar cells: toward suitable electronic energy levels and broad absorption. *Acc Chem Res* 2012;45:723–33.
- [4] Juan RS, Payne A-J, Welch GC, Eftaiha AF. Development of low band gap molecular donors with phthalimide terminal groups for use in solution processed organic solar cells. *Dyes Pigments* 2016. <http://dx.doi.org/10.1016/j.dyepig.2016.05.015>.
- [5] Sariciftci NS, Smilowitz L, Heeger AJ, Wudl F. Photoinduced electron transfer from a conducting polymer to buckminsterfullerene. *Science* 1992;258:1474–6.
- [6] Lin Y, Zhan X. Oligomer molecules for efficient organic photovoltaics. *Acc Chem Res* 2016;49:175–83.
- [7] Lin Y, Zhan X. Non-fullerene acceptors for organic photovoltaics: an emerging horizon. *Mater Horiz* 2014;1:470–88.
- [8] McAfee SM, Topple JM, Hill IG, Welch GC. Key components to the recent performance increases of solution processed non-fullerene small molecule acceptors. *J Mater Chem A* 2015;3:16393–408.
- [9] Nielsen CB, Holliday S, Chen HY, Cryer SJ, McCulloch I. Non-fullerene electron acceptors for use in organic solar cells. *Acc Chem Res* 2015;48:2803–12.
- [10] Kozma E, Catellani M. Perylene diimides based materials for organic solar cells. *Dyes Pigments* 2013;98:160–79.
- [11] Kang H, Zheng YQ, Jiang W, Xiao C, Wang JY, Pei J, et al. All-polymer solar cells based on PTACs/P3HT blends with large open-circuit voltage. *Dyes Pigments* 2013;99:1065–71.
- [12] Anthony JE. Small-molecule, nonfullerene acceptors for polymer bulk heterojunction organic photovoltaics. *Chem Mater* 2011;23:583–90.
- [13] Chochos CL, Tagmatarchis N, Gregorius VG. Rational design on n-type organic materials for high performance organic photovoltaics. *RSC Adv* 2013;3:7160–81.
- [14] Eftaiha AF, Sun J-P, Hill IG, Welch GC. Recent advances of non-fullerene, small molecular acceptors for solution processed bulk heterojunction solar cells. *J Mater Chem A* 2014;2:1201–13.
- [15] Lin Y, Wang J, Zhang ZG, Bai H, Li Y, Zhu D, et al. An electron acceptor challenging fullerenes for efficient polymer solar cells. *Adv Mater* 2015;27:1170–4.
- [16] Bin H, Zhang ZG, Gao L, Chen S, Zhong L, Xue L, et al. Non-fullerene polymer solar cells based on alkylthio and fluorine substituted 2D-conjugated polymers reach 9.5% efficiency. *J Am Chem Soc* 2016;138:4657–64.
- [17] Lin Y, Zhao F, He Q, Huo L, Wu Y, Parker TC, et al. High-performance electron acceptor with thiényl side chains for organic photovoltaics. *J Am Chem Soc* 2016;138:4955–61.
- [18] Lin Y, He Q, Zhao F, Huo L, Mai J, Lu X, et al. A facile planar fused-ring electron acceptor for as-cast polymer solar cells with 8.71% efficiency. *J Am Chem Soc* 2016;138:2973–6.
- [19] Gao L, Zhang ZG, Xue L, Min J, Zhang J, Wei Z, et al. All-polymer solar cells based on absorption-complementary polymer donor and acceptor with high power conversion efficiency of 8.27%. *Adv Mater* 2016;28:1884–90.
- [20] Meng D, Sun D, Zhong C, Liu T, Fan B, Huo L, et al. High-performance solution-processed non-fullerene organic solar cells based on selenophene-containing perylene bisimide acceptor. *J Am Chem Soc* 2016;138:375–80.
- [21] Sun D, Meng D, Cai Y, Fan B, Li Y, Jiang W, et al. Non-fullerene-acceptor-based bulk-heterojunction organic solar cells with efficiency over 7%. *J Am Chem Soc* 2015;137:11156–62.
- [22] Liu T, Meng D, Cai Y, Sun X, Li Y, Huo L, et al. High-performance non-fullerene organic solar cells based on a selenium-containing polymer donor and a twisted perylene bisimide acceptor. *Adv Sci* 2016. <http://dx.doi.org/10.1002/advs.201600117>.
- [23] Po R, Bianchi G, Carbonera C, Pellegrino A. “All that Glisters Is Not Gold”: an analysis of the synthetic complexity of efficient polymer donors for polymer solar cells. *Macromolecules* 2015;48:453–61.
- [24] Po R, Bernardi A, Calabrese A, Carbonera C, Corso G, Pellegrino A. From lab to fab: how must the polymer solar cell materials design change? –an industrial perspective. *Energy Environ Sci* 2014;7:925–43.
- [25] Machui F, Hosel M, Li N, Spyropoulos GD, Ameri T, Søndergaard RR, et al. Cost analysis of roll-to-roll fabricated ITO free single and tandem organic solar modules based on data from manufacture. *Energy Environ Sci* 2014;7:2792–802.
- [26] Burke DJ, Lipomi DJ. Green chemistry for organic solar cells. *Energy Environ Sci* 2013;6:2053–66.
- [27] Okamoto K, Zhang J, Housekeeper JB, Marder SR, Luscombe CK. C–H arylation reaction: atom efficient and greener syntheses of π-conjugated small molecules and macromolecules for organic electronic materials. *Macromolecules* 2013;46:8059–78.
- [28] Marrochi A, Facchetti A, Lanari D, Petrucci C, Vaccaro L. Current methodologies for a sustainable approach to π-conjugated organic semiconductors. *Energy Environ Sci* 2016;9:763–86.
- [29] Mercier LG, Leclerc M. Direct (Hetero)arylation: a new tool for polymer chemists. *Acc Chem Res* 2013;46:1597–605.
- [30] Wenczel-Delord J, Glorius F. C–H bond activation enables the rapid construction and late-stage diversification of functional molecules. *Nat Chem* 2013;5:369–75.
- [31] Liu SY, Li HY, Shi MM, Jiang H, Hu XL, Li WQ, et al. Pd/C as a clean and effective heterogeneous catalyst for C–C couplings toward highly pure semiconducting polymers. *Macromolecules* 2012;45:9004–9.
- [32] Hendsbee AD, Macaulay CM, Welch GC. Synthesis of an H-aggregated thiopheneethphthalimide based small molecule via microwave assisted direct arylation coupling reactions. *Dyes Pigments* 2014;102:204–9.
- [33] Shaabani A, Dabiri M, Bazgir A, Gharanjig K. Microwave-assisted rapid synthesis of 1,4-diketo-pyrrolo[3,4-c]pyrroles' derivatives under solvent-free conditions. *Dyes Pigments* 2006;71:68–72.
- [34] McAfee SM, Topple JM, Payne AJ, Sun JP, Hill IG, Welch GC. An electron-deficient small molecule accessible from sustainable synthesis and building blocks for use as a fullerene alternative in organic photovoltaics. *ChemPhysChem* 2015;16:1190–202.
- [35] McAfee SM, McCahill JSJ, Macaulay CM, Hendsbee AD, Welch GC. Utility of a heterogeneous palladium catalyst for the synthesis of a molecular semiconductor via Stille, Suzuki, and direct heteroarylation cross-coupling reactions. *RSC Adv* 2015;5:26097–106.
- [36] McAfee SM, Cann JR, Josse P, Blanchard P, Cabanetos C, Welch GC. The optimization of direct heteroarylation and Sonogashira cross-coupling reactions as efficient and sustainable synthetic methods to access π-conjugated materials with near-infrared absorption. *ACS Sustain Chem Eng* 2016;4:3504–17.
- [37] Hendsbee AD, Sun J-P, Rutledge LR, Hill IG, Welch GC. Electron deficient diketopyrrolopyrrole dyes for organic electronics: synthesis by direct arylation, optoelectronic characterization, and charge carrier mobility. *J Mater Chem A* 2014;2:4198–207.
- [38] Broll S, Nübling F, Luzio A, Lentzas D, Komber H, Caironi M, et al. Defect analysis of high electron mobility diketopyrrolopyrrole copolymers made by direct arylation polycondensation. *Macromolecules* 2015;48:7481–8.
- [39] Areephong J, Hendsbee AD, Welch GC. Facile synthesis of unsymmetrical and π-extended furan-diketopyrrolopyrrole derivatives through C–H direct (hetero)arylation using a heterogeneous catalyst system. *New J Chem* 2015;39:6714–7.
- [40] Wallquist O, Lenz R. 20 Years of DPP pigments—future perspectives. *Macromol Symp* 2002;187:617–30.
- [41] Qu S, Tian H. Diketopyrrolopyrrole (DPP)-based materials for organic photovoltaics. *Chem Commun* 2012;48:3039–51.
- [42] Nielsen CB, Turbiez M, McCulloch I. Recent advances in the development of semiconducting DPP-containing polymers for transistor applications. *Adv Mater* 2013;25:1859–80.
- [43] Grzybowski M, Gryko DT. Diketopyrrolopyrroles: synthesis, reactivity, and optical properties. *Adv Opt Mater* 2015;3:280–320.
- [44] Kaur M, Choi DH. Diketopyrrolopyrrole: brilliant red pigment dye-based fluorescent probes and their applications. *Chem Soc Rev* 2015;44:58–77.
- [45] Liu SY, Shi M, Huang J, Jin Z, Hu X, Pan J, et al. C–H activation: making diketopyrrolopyrrole derivatives easily accessible. *J Mater Chem A* 2013;1:2795–805.
- [46] Heeger AJ. Semiconducting polymers: the third generation. *Chem Soc Rev* 2010;39:2354–71.
- [47] Yu Y, Yang F, Ji Y, Wu Y, Zhang A, Li C. A perylene bisimide derivative with a LUMO level of -4.56 eV for non-fullerene solar cells. *J Mater Chem C* 2016;4:4134–7.
- [48] Kotowski D, Luzzati S, Scavia G, Cavazzini M, Bossi A, Catellani M, et al. The effect of perylene diimides chemical structure on the photovoltaic performance of P3HT/perylene diimides solar cells. *Dyes Pigments* 2015;120:57–64.
- [49] Lin Y, Cheng P, Li Y, Zhan X. A 3D star-shaped Non-fullerene acceptor for solution-processed organic solar cells with a high open-circuit voltage of 1.18 V. *Chem Commun* 2012;48:4773–5.
- [50] Lin Y, Li Y, Zhan XA. Solution-processable electron acceptor based on dibenzosilole and diketopyrrolopyrrole for organic solar cells. *Adv Energy Mater* 2013;3:724–8.
- [51] Li S, Yan J, Li CZ, Liu F, Shi M, Chen H, et al. A non-fullerene electron acceptor

- modified by thiophene-2-carbonitrile for solution-processed organic solar cells. *J Mater Chem A* 2016;4:3777–83.
- [52] Li S, Liu W, Shi M, Mai J, Lau TK, Wan J, et al. Spirobifluorene and diketopyrrolopyrrole moieties based non-fullerene acceptor for efficient and thermally stable polymer solar cells with high open-circuit voltage. *Energy Environ Sci* 2016;9:604–10.
- [53] Wu XF, Fu WF, Xu Z, Shi M, Liu F, Chen HZ, et al. Spiro linkage as an alternative strategy for promising nonfullerene acceptors in organic solar cells. *Adv Funct Mater* 2015;25:5954–66.
- [54] Zhang X, Lu Z, Ye L, Zhan C, Hou J, Zhang S, et al. A potential perylene diimide dimer-based acceptor material for highly efficient solution-processed nonfullerene organic solar cells with 4.03% efficiency. *Adv Mater* 2013;25:5791–7.
- [55] Li H, Earmme T, Ren G, Saeki A, Yoshikawa S, Murari NM, et al. Beyond fullerenes: design of nonfullerene acceptors for efficient organic photovoltaics. *J Am Chem Soc* 2014;136:14589–97.
- [56] Lin Y, Wang Y, Wang J, Hou J, Li Y, Zhu D, et al. A star-shaped perylene diimide electron acceptor for high-performance organic solar cells. *Adv Mater* 2014;26:5137–42.
- [57] Liu Y, Mu C, Jiang K, Zhao J, Li Y, Zhang L, et al. A tetraphenylethylene core-based 3D structure small molecular acceptor enabling efficient nonfullerene organic solar cells. *Adv Mater* 2015;27:1015–20.
- [58] Liu SY, Wu CH, Li CZ, Liu SQ, Wei KH, Chen HZ, et al. A tetraperylene diimides based 3D nonfullerene acceptor for efficient organic photovoltaics. *Adv Sci* 2015;2:1500014.
- [59] Lee J, Singh R, Sin DH, Kim HG, Song KC, Cho K. A nonfullerene small molecule acceptor with 3D interlocking geometry enabling efficient organic solar cells. *Adv Mater* 2016;28:69–76.
- [60] Tong H, Hong YN, Dong YQ, Haussler M, Lam JYW, Li Z, et al. Fluorescent “light-up” bioprobes based on tetraphenylethylene derivatives with aggregation-induced emission characteristics. *Chem Commun* 2006;3705–7.
- [61] Hong YN, Lam JYW, Tang BZ. Aggregation-induced emission: phenomenon, mechanism and applications. *Chem Commun* 2009;4332–53.
- [62] Anastas PT, Kirchhoff MM. Origins, current status, and future challenges of green chemistry. *Acc Chem Res* 2002;35:686–94.
- [63] Burckstummer H, Weissenstein A, Bialas D, Würther F. Synthesis and characterization of optical and redox properties of bithiophene-functionalized diketopyrrolopyrrole chromophores. *J Org Chem* 2011;76:2426–32.
- [64] Liu SY, Fu WF, Xu JQ, Fan CC, Jiang H, Shi M, et al. A direct arylation-derived DPP-based small molecule for solution-processed organic solar cells. *Nanotechnology* 2014;25:014006.
- [65] Liu SY, Liu WQ, Xu JQ, Fan CC, Fu WF, Ling J, et al. Pyrene and diketopyrrolopyrrole-based oligomers synthesized via direct arylation for OSC applications. *ACS Appl Mater Interfaces* 2014;6:6765–75.
- [66] Liu SY, Jung JW, Li CZ, Huang J, Zhang J, Chen H, et al. Three-dimensional molecular donors combined with polymeric acceptors for high performance fullerene-free organic photovoltaic devices. *J Mater Chem A* 2015;3:22162–9.
- [67] Viterisi A, Gispert-Guirado F, Ryan JW, Palomares E. Formation of highly crystalline and textured donor domains in DPP(TBFu)₂:PC₇₁BM SM-BHJ devices via solvent vapour annealing: implications for device function. *J Mater Chem* 2012;22:15175–82.
- [68] Walker B, Tamayo AB, Dang XD, Zalar P, Seo JH, Garcia A, et al. Nanoscale phase separation and high photovoltaic efficiency in solution-processed, small-molecule bulk heterojunction solar cells. *Adv Funct Mater* 2009;19:3063–9.
- [69] Fréchet JM, Thompson BC. Polymer-fullerene composite solar cells. *Angew Chem Int Ed* 2008;47:58–77.
- [70] Walker B, Han X, Kim C, Sellinger A, Nguyen T-Q. Solution-processed organic solar cells from dye molecules: an investigation of diketopyrrolopyrrole: vinazene heterojunctions. *ACS Appl Mater Interfaces* 2012;4:244–50.
- [71] Ni W, Li M, Kan B, Liu F, Wan X, Zhang Q, et al. Fullerene-free small molecule organic solar cells with a high open circuit voltage of 1.15 V. *Chem Commun* 2016;52:465–8.
- [72] Zhang J, Zhang X, Li G, Xiao H, Li W, Xie S, et al. A nonfullerene acceptor for wide band gap polymer based organic solar cells. *Chem Commun* 2016;52:469–72.